Shape Optimization Of Instrument Panel Components For Crashworthiness Using Distributed Computing

Alex Akkerman*, Mike Burger‡, Bob Kuhn†, Hrabri Rajic†, Nielen Stander‡, Ravi Thyagarajan*

* Ford Motor Company
† Kuck & Associates, Inc.
‡ Livermore Software Technology Corp.

Contact:

Robert Kuhn
Kuck & Associates, Inc.
1906 Fox Drive
Champaign, IL 61820
+1 217-356-2288
kuhn@kai.com

Abbreviations:

D_{LK}, D_{RK} -- Displacement of the Left and Right Knee
D_{LBT}, D_{LBF}, D_{LBB} -- Depth of Left Bracket: Top, Front, and Bottom
EA – Energy Absorption
F_{LK}, F_{RK} – Force on Left and Right Knee
G_{RB}, G_{LB}, G_{KB} -- Gauge of Left and Right Bracket and Knee Bolster
IP – Instrument Panel
$KE_{initial}$, KE_{final} – Total Kinetic Energy, initial and final
R_Y, R_{RB} --Cross-section Radius of Steering Yoke,Radius Right EA Hole
W_{RB}, $W_{LB,}W_{LBF}$ -- Width Right and Left Bracket and Left Bracket Flange

Keywords:
Crashworthiness, Design Optimization, Distributed Computing, Energy Management, Knee Bolster, Parametric Preprocessing, Shape Optimization.

ABSTRACT

The ability to quickly design new vehicles with optimal crashworthiness is a goal of automotive manufacturers. This paper takes steps towards that goal by automating manual design iterations. The crashworthiness of an instrument panel was enhanced using LS-OPT and LS-DYNA. It is shown that:

- LS-OPT can modify the shape of non-styled parts in the instrument panel in order to enhance its crashworthiness by using a parametric preprocessor, e.g. TrueGrid®.
- The design was generated several times faster than with manual methods. LS-OPT generated and executed LS-DYNA runs without need for manual result analysis.
- The dramatic increase in the size of the design space caused by shape optimization was managed efficiently by LS-OPT.
- The cost of obtaining these designs can be reduced by using distributed computing to explore the design space on workstations which would otherwise be underutilized.

INTRODUCTION

The automotive instrument panel (IP) has evolved over time to become one of the most complex subsystems in today's automobile (Jira, 1996), both from an appearance and functionality viewpoint. Not only does it lend a distinctive character to the interior of an automobile from an aesthetic point of view, it must also house beneath the styled surface several components required for functional reasons. Some examples of these are cross-vehicle structure, steering column supports, climate control system, electronic modules and wiring, airbags, and a knee bolster system. Of particular significance to this paper is the knee bolster portion of an IP, which is designed to perform several functions (Kulkarni, 1998). Most notably it provides the first contact surface for the knees in a frontal impact situation. Also, it participates in cushioning and directing the knees and in energy management of the lower torso of the occupant.

Design variables for problems of this type can create a very large design space that the engineer must explore. Typical parameters are:

- Gauge and modulus of the material in the energy absorption (EA) brackets,
- Gauge and modulus of the knee bolster material,
- Steering column isolator cross-section radius, and
- Lightening holes and flange depth in the EA brackets.

In the previous European LS-DYNA Users Group Meeting a paper was presented using LS-OPT to optimize the gauges and materials of these components, the first two types of parameters. (Akkerman, 1999). Since the design problem was small, second order response surfaces could be used to construct a trade-off diagram of maximum knee force versus intrusion.

In the present paper the search of a much larger design space, covering all four parameter types, was automated. Although the response variables and objective function remain basically the same, the number of design variables increased from 3 to 11. This dramatically enlarged the design space precluding the use of complex design surfaces.

Because of the additional design complexity two major features are introduced:

® True*Grid* is a registered trademark of XYZ Scientific Applications, Inc., http://www.truegrid.com.

- A parametric preprocessor, TrueGrid, to allow geometric modeling.
- A successive linear approximation procedure to reduce the number of simulations.

Although the latter method is linear versus the quadratic method used previously, it is shown that only three or four iterations are required for convergence. This can be achieved by reducing the size of the region of interest in the design space. (Stander, 2000)

Computationally, it was demonstrated that the workstation cluster environment was just as easy to use as the compute server when running LS-OPT. Given the cost and availability of unused computer cycles, the distributed LS-OPT version is a significant step forward.

Figure 1. Typical instrument panel prepared for a “Bendix” component test.

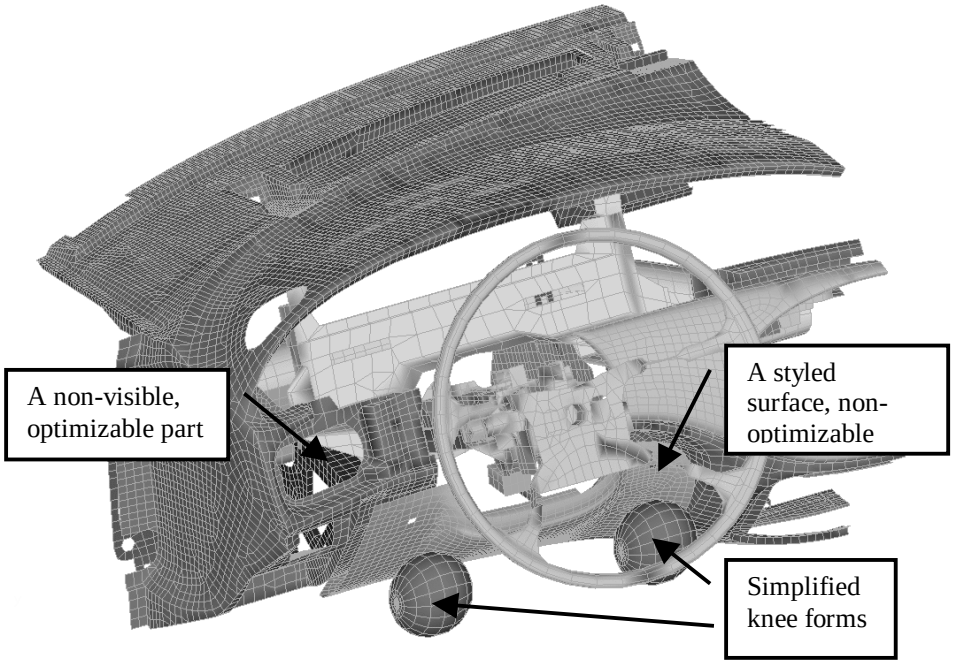

General Problem Statement

Figure 1 shows the finite element model of a typical automotive IP. For model simplification and reduced per-iteration computational times, only the driver's side of the IP is used in the analysis as shown, and consists of around 25,000 shell elements with 60 PIDs and 11 materials. Symmetry boundary conditions are assumed at the centerline, and to simulate a bench component "Bendix" test, body attachments are assumed fixed in all 6 directions. Also shown in Figure 1 are simplified knee forms which move in a direction as determined from prior physical tests. The mass (17.5 kg each) and initial velocity (6.62 m/sec) of the knees are tuned to reflect a predetermined lower torso energy (770 J) that is typically managed by an IP, most of which is borne by the knee bolster system shown in Figure 2. As shown in the figure, this system is composed of a knee bolster (steel, plastic or both) that also serves as steering column cover whose surface is styled and should not be changed, two EA brackets (usually steel) attached to the cross vehicle IP structure that absorb a significant portion of the lower torso energy of the occupant by deforming appropriately, as shown in Figure 3. Sometimes, a steering column isolator (also known as a yoke) may be used as part of the knee

bolster system to delay the wrap-around of the knees around the steering column. The last three components are non-visible and hence their shape can be optimized. Some of the design variables are shown in Figure 2.

The simulation is carried out for a 40 ms duration by which time the knees have been brought to rest. It may be mentioned here that the Bendix component test is used mainly for knee bolster system development; for certification purposes, a different physical test representative of the full vehicle is performed. Since the simulation used herein is at a subsystem level, the results reported here may be used mainly for illustration purposes.

Figure 2. Typical major components of a knee bolster system.

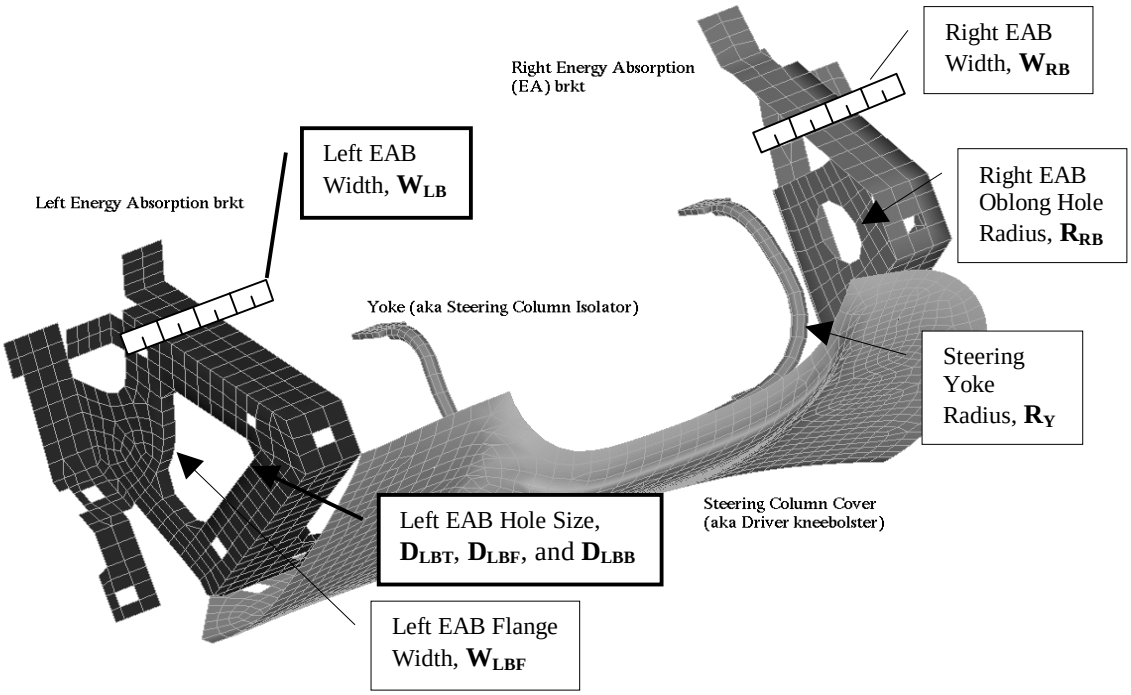

Defining the Design Space

The gauge of the EA brackets and the knee bolster are firstly defined. The range of materials and their gauges is limited by manufacturing to specific values, but to explore freely for an optimum design, any gauge in a range is assumed to be available. Table 1 shows which part gauges were varied and the range over which they were varied.

Table 1. Part gauges that were varied and the design space of the optimization.

Description	Lower Limit (mm)	Variable	Upper Limit (mm)	Baseline (mm)	Baseline Material
Left Bracket Gauge	0.7	$\leq G_{RB} \leq$	3	1.1	Steel
Right Bracket Gauge	0.7	$\leq G_{LB} \leq$	3	1.1	Steel
Knee Bolster Gauge	1	$\leq G_{KB} \leq$	6	3.5	SMC

The EA brackets and yoke were modeled with steel in all the analyses. The knee bolster was modeled with SMC (Sheet Molding Compound).

To specify a shape optimization problem, we start with a baseline design and specify how its geometry may be varied. The complexity of doing this depends on the part being optimized. Figure 2 shows the parameterization of the three parts to be optimized in this design. The yoke is simplest to describe. One design variable, the cross-section radius of the yoke, $\mathbf{R_Y}$, may be varied. It is clear how to specify it as a constraint:

Table 2. Yoke shape design space.

Description	Lower Limit (mm)	Variable	Upper Limit (mm)	Baseline (mm)	Baseline Material
Yoke Radius	4	$\leq \mathbf{R_Y} \leq$	10	7	Steel

Now, consider the right EA bracket. The shape optimization will restrict itself to two areas:

- **Right EA Hole Radius** -- The hole in the right EA bracket has been modeled as an oblong hole. The radius of the hole is one design variable, $\mathbf{R_{RB}}$. The out-of-round dimension of the hole was arbitrarily fixed and is not considered a design variable.
- **Right EA Flange Width** -- Around the outside of the bracket the metal has been folded at 90 degrees to make a mounting surface and to provide flange stiffness. The width of the flange is $\mathbf{W_{RB}}$.

For the left EA bracket, the shape optimization will restrict itself to three areas:

- **Size and shape of the hole** -- There are three design variables, $\mathbf{D_{LBT}}$, $\mathbf{D_{LBF}}$, $\mathbf{D_{LBB}}$. These correspond to the flange depths in the bracket plane for 3 of the 4 primary edges of the left EA bracket, the top, the front, and the bottom, as seen from the driver's position. The depth of the back of bracket is currently fixed.
- **Inner Flange Width** -- The hole in the left EA bracket has been folded inward to form a metal rim which acts to stiffen the bracket. The width of the flange is a design variable, $\mathbf{W_{FLB}}$.
- **Width of the bracket** -- As with the right AE bracket, the outside of the bracket has been folded at 90 degrees. The width of the flange is $\mathbf{W_{LB}}$.

Fillets to round the four sides of the hole have not been used because they are not likely to have global effects.

The shape variables are summarized in the following table:

Table 3. Left and right energy absorption bracket shape design space.

Description	Lower Limit (mm)	Variable	Upper Limit (mm)	Baseline (mm)
Right EA Hole Radius	10	$\leq \mathbf{R_{RB}} \leq$	25	15
Right EA Width	20	$\leq \mathbf{W_{RB}} \leq$	40	32
Left EA Depth Top	20	$\leq \mathbf{D_{LBT}} \leq$	40	28.3
Left EA Depth Front	20	$\leq \mathbf{D_{LBF}} \leq$	40	27.5
Left EA Depth Bottom	20	$\leq \mathbf{D_{LBB}} \leq$	40	22.3
Left EA Inner Flange Width	5	$\leq \mathbf{W_{LBF}} \leq$	15	7
Left EA Width	20	$\leq \mathbf{W_{LB}} \leq$	40	32

OPTIMIZATION PROBLEM CONSTRAINTS

For optimal occupant kinematics, it is essential that knee intrusion into the IP be limited to desired values. Upper bounds of the left and right knee displacements, $\mathbf{D_{LK}}$ and $\mathbf{D_{RK}}$, are used to limit knee intrusions. In this case the variables were constrained to be **less than 115 mm**.

Figure 3. Knee bolster system after deformation.

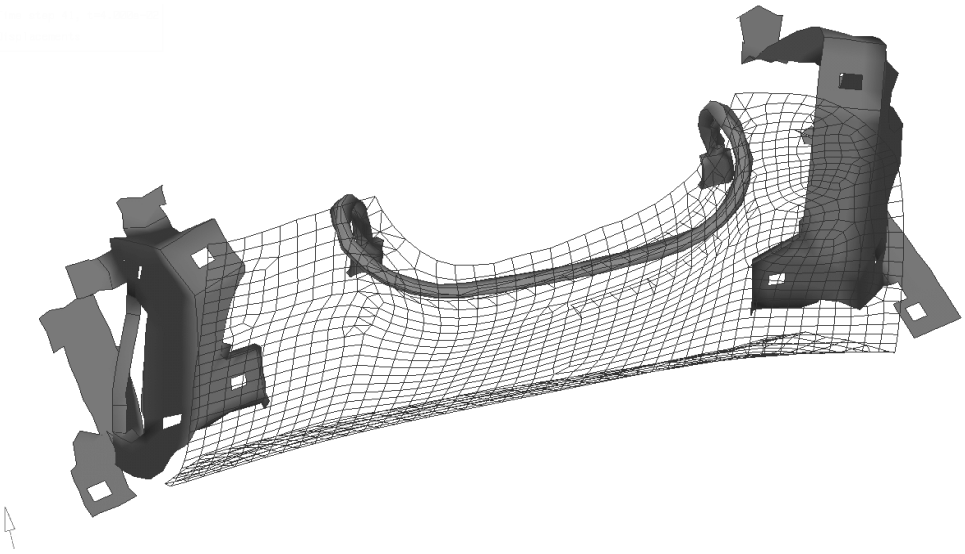

Optimization Problem Objective

In general, the primary object of knee bolster crashworthiness engineering is to minimize the forces on the occupant to specific program targets within the limits of the design envelope. Therefore, the primary optimization criterion is to minimize the force on the occupant's left and right knees, $\mathbf{F_{LK}}$ and $\mathbf{F_{RK}}$. The selection of a low force constraint value forced the optimization strategy to be minimize the maximum knee force subject to the constraints above.

Objective Function: min (max (F_{LK} , F_{RK}))

The maximization considers both the knee forces over time. The knee forces have been filtered, SAE 60 Hz, to improve the approximation accuracy.

Design Summary Table

Table 4 lists the design variable values and responses for: the baseline design, Figures 2 and 3; the shape optimized design, Tables 1 through 3; and the gauge-only optimization, Table 1. Because there were some design changes in the structure, the baseline design responses are different from those reported in the previous paper (Akkerman, 1999).

Table 4. Baseline design characteristics.

Parameter	Baseline	Shape Optimized	Gauge Only Optimized
Left Bracket Gauge, G_{RB}	1.1	0.84	0.99
Right Bracket Gauge, G_{LB}	1.1	0.7	0.86

Knee Bolster Gauge, G_{KB}	3.5	6	5.63
Yoke Cross-Section Radius, R_Y	7	4	7
Right EA Hole Radius, R_{RB}	15	13.14	15
Right EA Width, W_{RB}	32	34.39	32
Left EA Depth Top, D_{LBT}	28.3	26.23	28.3
Left EA Depth Front, D_{LBF}	27.5	31.5	27.5
Left EA Depth Bottom, D_{LBB}	22.3	34.02	22.3
Left EA Inner Flange Width, W_{LBF}	7	14.25	7
Left EA Width, W_{LB}	32	27.87	32
Maximum Left Knee Force	7625 N	6602 N	7821 N
Maximum Right Knee Force	9458 N	6293 N	7850 N
Maximum Left Knee Displacement	92 mm	97.3 mm	92.7 mm
Maximum Right Knee Displacement	88 mm	95.41 mm	80.7 mm

Figure 4. Views of the smallest and largest shapes in the design space.

(a) Smallest left bracket.

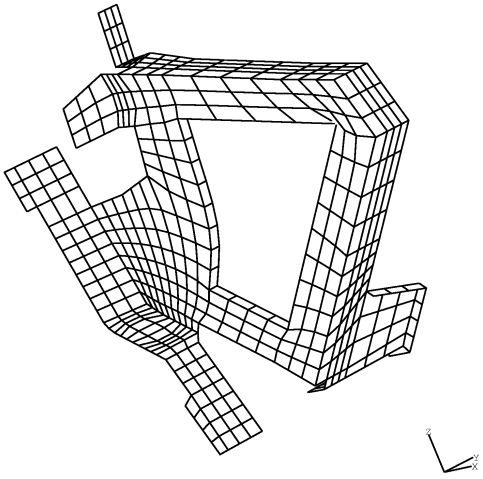

(b) Smallest right bracket.

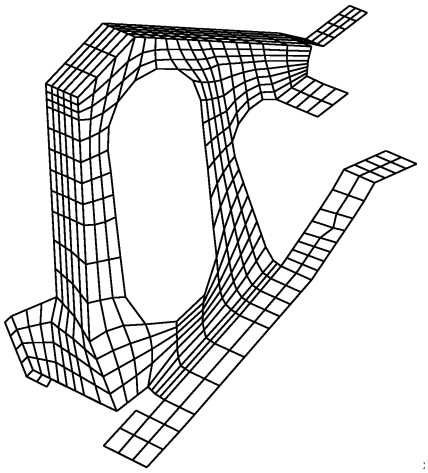

(a) Largest left bracket.

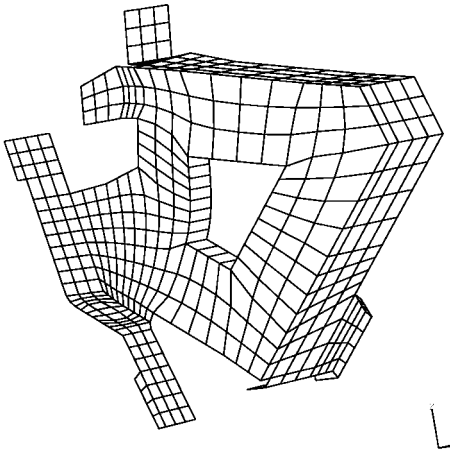

(b) Largest right bracket.

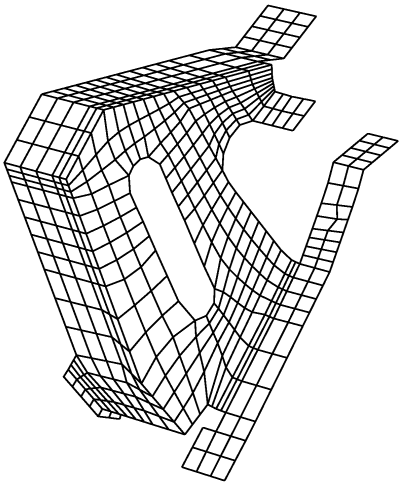

Specifying Shape Optimization Input Files with TrueGrid

LS-OPT will call a user-selected preprocessor before each LS-DYNA run. Before calling the preprocessor, it substitutes the design variable values for their symbolic parameters in the preprocessor input file. This causes the preprocessor to customize the design for the selected design point. We chose to use TrueGrid for preprocessing the design for three reasons:

- It has more parametric capability than other parametric modeling programs. With TrueGrid any piece of data can be parameterized to be an LS-OPT design variable.
- The meshing can be parameterized to adapt to shape changes.
- TrueGrid specializes in hexahedral meshing which is important for high quality elements.

The original LS-DYNA input file for the IP was modified to prepare it for shape optimization in several steps:

1) TrueGrid was used to produce surface geometry from the original LS-DYNA input. This was a critical step that separated the geometry from the other LS-DYNA input parameters. In the extracted pure geometry it was necessary to preserve the fixed parts of the baseline design:
   - The Bendix occupant impact model,
   - The knee bolster and IP which are styled surfaces,
   - The attachment points between the parts, and
   - The mounting of the IP system which is considered clamped in the Bendix test.

2) From the new surface geometry TrueGrid created the components to be shape optimized with parameterized variables. This included the 11 parameters that are varied in this optimization problem. LS-OPT automatically appended the fixed part of the model to the TrueGrid output before simulation.

Preparing the parameterized input file for the IP according to the parameters above took about 8 hours for a skilled user of TrueGrid. Figure 4 illustrates the range of designs in the design space in terms of the geometry of the smallest and largest brackets.

Computational Environment

LS-OPT generated 19 LS-DYNA design points for each iteration. This number is based on the number of design variables with a provision for over-sampling the design space (Roux, 1999). Three iterations were needed for convergence of this problem, so the total number of simulations including a final check run was 58.

Runs were made on two computational environments: a server and a workstation network:

1. HP V-class running 10 processors simultaneously. Each LS-DYNA run took about 3.5 hours on one processor.
2. The workstation cluster consisted of a network of 4 dual-processor Intel systems running Windows-NT for LS-DYNA runs and an SGI O200 as follows:
   2 processors on a 550MHz dual PIII Xeon / NT (Blaze)
   1 processor on a 500MHz dual PIII Xeon / NT (Rum)
   2 processors on a 450MHz dual PII Xeon / NT (Tropical)
   2 processors on a 450MHz dual PII Xeon / NT (Zpro)
   2 processors on an O200 / IRIX (Gemini)
   Each LS-DYNA job took between 3.5 and 4.5 hours. LS-OPT ran on the O200.

The Application Distributor software in LS-OPT managed sending out LS-DYNA runs across the cluster to these systems and bringing back the relevant data. Executing LS-OPT software was identical in both environments with the exception of requiring workstations in the network environment to be identified as available for executing LS-DYNA jobs.

Figure 5. Maximum knee forces on each iteration.

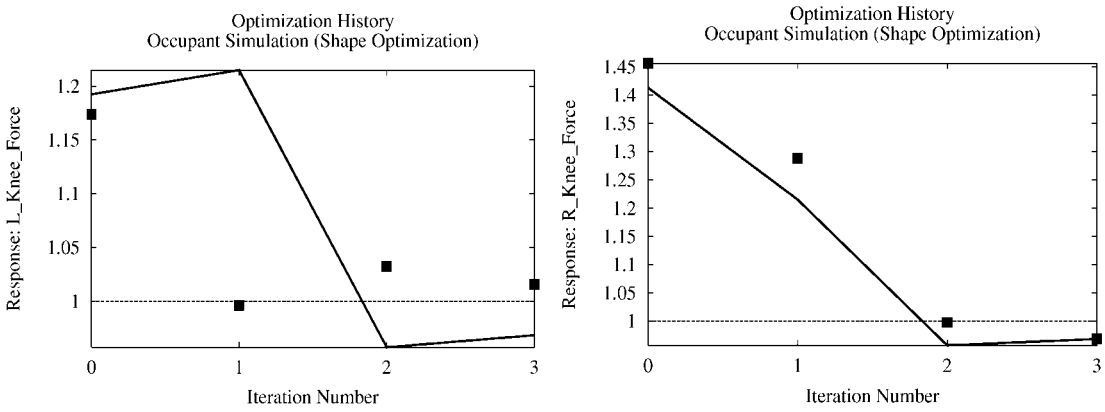

Figure 6. Trade-off between maximum knee force and displacement.

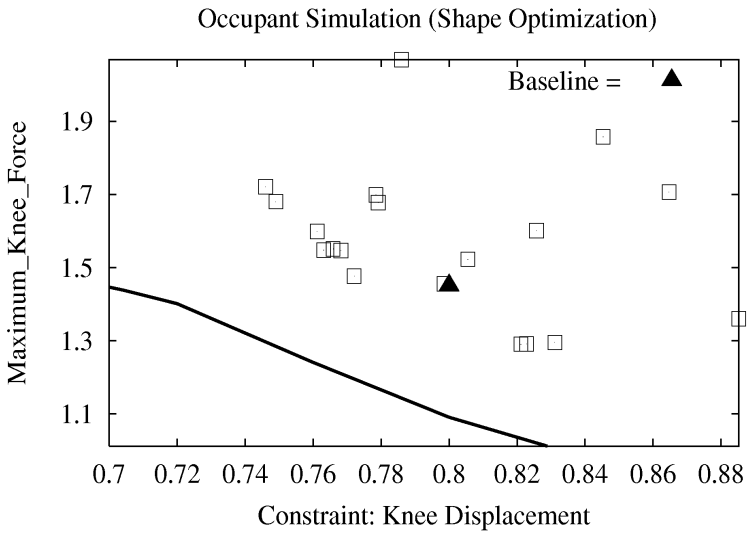

DISCUSSION OF RESULTS

Figure 5 depicts the optimization history of the knee forces when normalized to 6500N and Table 4 summarizes the optimized design. Despite the large design space, it is shown that in basically two iterations the maximum force was reduced to its minimum value. The optimization brought the maximum simulated knee force down from 9457 to 6602, an improvement of 30% in a simulation of the Bendix test. However, it must be mentioned that because this analysis is based on a single size occupant, a defined vehicle environment, and a single test mode, more simulations would be necessary to determine the overall effectiveness of this design. (In the future, the multi-case feature of LS-OPT may be used to incorporate

multiple simulation cases in the same design.) The server computational environment and the cluster of workstations environment produced knee forces that were less than 1% different on the optimized design although the values of the design variables for the optimized designs were different. This suggests that, due to the many design variables in this problem, there are multiple mechanisms which result in the same minimal knee forces.

Figure 7. Predicted versus computed force and displacement for the left knee.

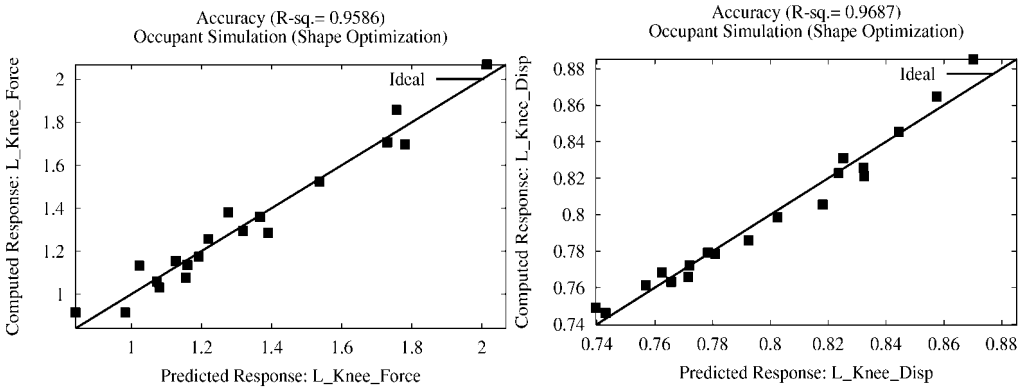

Figure 8. Size of key design variables during shape optimization.

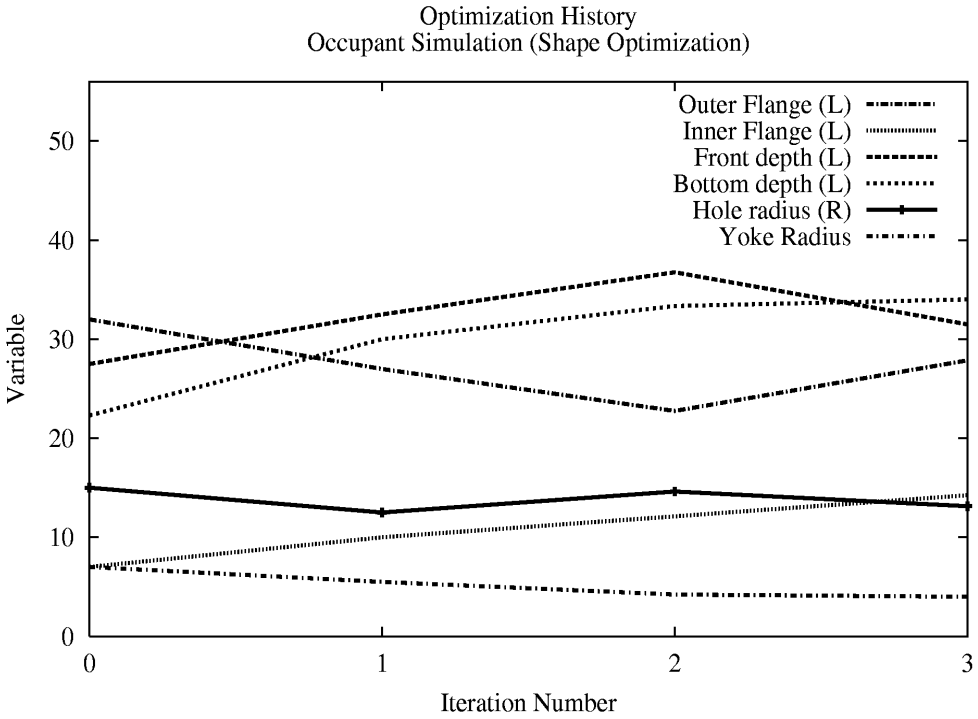

Figure 6 shows the approximate trade-off between normalized maximum knee force and knee displacement normalized to 115mm. It is shown that the force increases with a constrained displacement. As expected, no design points occur inside the predicted tradeoff curve, confirming relative accuracy of the design problem. A further investigation into the accuracy of the first design approximation (Figure 7) also confirms this aspect. In this over-sampled

approximation, all of the design points are close to their predicted value over a wide range of variation.

Figure 8 illustrates the value of shape optimization. Several dimensions were changed significantly from the baseline design:

- The internal flange on the left EA bracket increased to the maximum allowed size.
- The dimensions of the hole in left EA bracket grew in some dimensions and shrunk in other dimensions.
- The yoke cross-section radius was made smaller. And,
- The right EA bracket hole size changed very little.

To quantify the effect of shape optimization, the baseline design was optimized with only the gauge design variables active. The maximum simulated knee forces converged at 7852. Thus shape optimization in the configuration we tested appeared to have contribute 19% to the results described above.

Final checks confirm the success of the process:

- The final kinetic energy for the optimum design was determined to be 7% of the initial energy, indicating that the design did absorb most of the impact energy.
- Figure 9 shows the filtered (60Hz) and unfiltered knee forces of the final design. Note that the peaks, which become active in the design process, occur at different times.
- It was also observed that the yoke deformations were quite similar in the baseline and optimized designs leading to the conclusion that column isolation performance was also comparable in the two designs.

Figure 9. Left and right knee forces in the optimized design over simulation time.

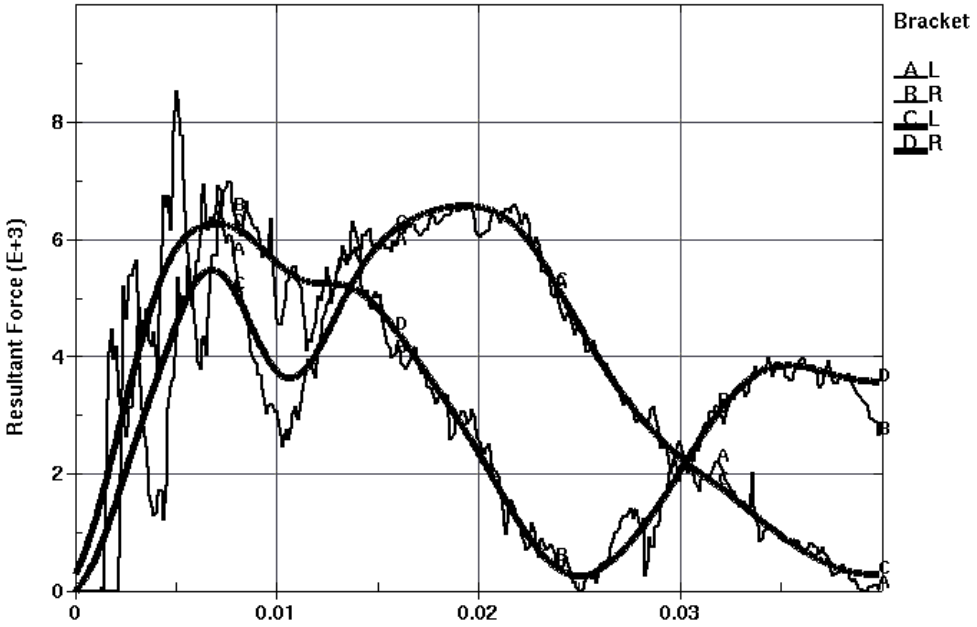

Distributed Computation

Each LS-OPT iteration of this optimization consisted of 19 LS-DYNA jobs. LS-OPT has the capability to execute independent jobs on an SMP server or to distribute jobs across the internet to available workstations or servers. Both programs run the same way to the user. Figure 10 illustrates what happens behind the scenes to allow an LS-OPT user to use a network of different types of systems transparently. The Application Distributor software library creates proxy processes on the distributor computer running LS-OPT. They communicate with Task Proxies on each available task server. Both the LS-OPT and the Local Task think they are communicating to each other on the same system.

LS-OPT parallel processing performance was comparable on the server and on the workstations. The granularity of LS-OPT parallelism is extremely coarse -- each task is a few hour LS-DYNA run. Data communication is relatively low -- files were copied to and from local working directories just as on LS-OPT server.

LS-OPT running in distributed mode provides greater flexibility, better productivity, and more consistent results:

- Greater Flexibility – Any configuration of workstation and servers with available time can be used while the optimization is being run.
- Better Productivity – LS-OPT's optimization method can search and evaluate more designs faster than an engineer can.
- Consistent Results – Creating many single-processor LS-DYNA jobs to use available systems reduces numerical differences that are inevitable in parallel LS-DYNA runs. Thus, one source of "noise" in simulations is eliminated.

Monitoring runs in the distributed computational environment is more interesting than in the server case. On the server, LS-OPT periodically shows the status of the LS-DYNA jobs being run. This is important for the person running LS-OPT and it is preserved in the distributed environment. In addition, for the distributed environment, the users of the workstations and servers contributing to the run want to monitor and control how much of their systems are being utilized by LS-OPT. In distributed mode, users can control the LS-OPT computational environment with an interactive monitor and control program. Being a super user or a system manager is not necessary.

Figure 10. Distributed execution environment.

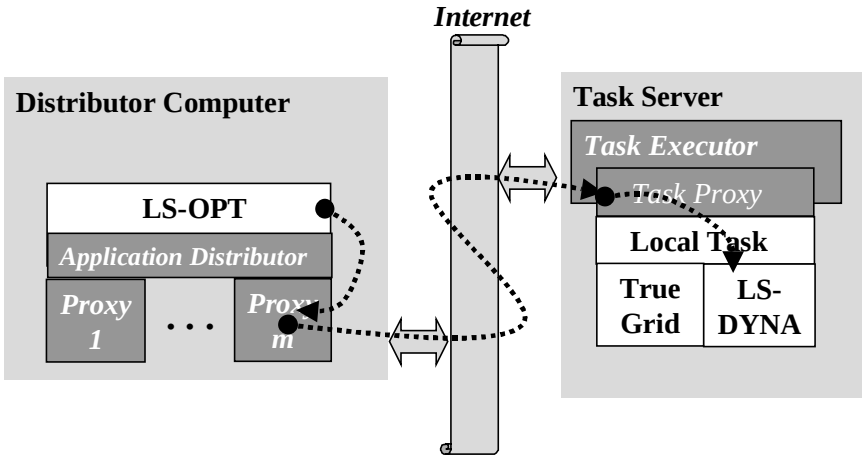

CONCLUSIONS

LS-OPT can be used to modify part gauges and shapes in the instrument panel in order to enhance its crashworthiness. LS-OPT was relatively easy to use for the optimizations performed.

- LS-OPT is a useful tool for finding an optimum solution to an IP crashworthiness simulation.
- The optimization can be performed concurrently for many simultaneously varying gauge and shape parameters.
- The predicted LS-OPT results were all well within the acceptable levels of correlation with the actual LS-DYNA runs for the same design parameters.

It was seen that using design optimization tools can leverage the creativity of the engineer by allowing him to explore new design options while using computer time to thoroughly analyze the well known design space.

Computationally, LS-OPT on workstations enables more automotive engineers to use this productivity tool. In addition, it offers computer users a very effective means to use workstation idle cycles.

ACKNOWLEDGEMENTS

We would like to send our greatest thanks and appreciation to Kumar Kulkarni of Ford Motor Company who built the finite element model used in this study.

REFERENCES

A. AKKERMAN, B. KUHN, H. RAJIC, N. STANDER, R. THYAGARAJAN, “Optimization of Instrument Panel Crashworthiness”, 2nd European LS-DYNA Users Group Meeting, May, 1999.

JIRA, J., KULKARNI, K., and THYAGARAJAN, R., "Deformation Control in Automotive Instrument Panels Exposed to High Sunload Temperatures With the Use of Unique Cowltop Attachments", International Body Engineering Conference,1996, Interior and Safety Systems, Detroit, MI, Oct 1996.

KULKARNI, K., and THYAGARAJAN, R., "A Brief Look at Instrument Panel Knee Bolster Designs and Materials", 1998 Regional Technical Conference of Society of Plastics Engineers, Detroit, MI, May 1998.

ROUX, W.J., STANDER, N., and HAFTKA, R., “Response Surface Approximations for Structural Optimizations”, International Journal for Numerical Methods in Engineering, Vol. 42, pp. 517-534, 1999.

STANDER, N., “Crashworthiness Design Optimization Using LS-OPT and Full-Model LS-DYNA Analyses”, LS-DYNA Users Conference, Japan, 1998.

STANDER, N., REICHERT, R, and FRANK, T. “Optimization of Nonlinear Dynamical Problems Using Successive Linear Approximations in LS-OPT”, 6th International LS-DYNA Users Conference, Dearborn, MI, April 9-11, 2000.

STANDER, N., ROUX, W., PATTABIRAMAN, S., and DHULIPUDI, R., “The Application of LS-OPT to Design Optimization Problems in Nonlinear Dynamics Using LS-DYNA”, 5th International LS-DYNA Users Conference, Detroit, MI, September 1998.